

New-Onset Psychosis Associated With a Lesion Localized in the Rostral Tectum: Insights Into Pathway-Specific Connectivity Disrupted in Psychosis

Eleftheria Koropouli^{*1,2}, Nikos Melanitis³, Vasileios I. Dimitriou¹, Asimina Grigoriou¹, Efstratios Karavasilis⁴, Konstantina S. Nikita³, Elias Tzavellas¹, and Thomas Paparrigopoulos¹

¹First Department of Psychiatry, Aiginition Hospital, National and Kapodistrian University of Athens School of Medicine, Athens, Greece; ²Present address: First Department of Neurology, Aiginition Hospital, National and Kapodistrian University of Athens School of Medicine, Athens, Greece; ³School of Electrical and Computer Engineering, National Technical University of Athens, Athens, Greece; ⁴Second Department of Radiology, Attikon Hospital, National and Kapodistrian University of Athens School of Medicine, Athens, Greece

*To whom correspondence should be addressed; First Department of Neurology, Aiginition Hospital, National and Kapodistrian University of Athens, Vasilissis Sofias Avenue 72–74, Athens, Attica 11528, Greece, e-mail: ekoropou@med.uoa.gr.

Objective: To investigate pathway-specific connectivity disrupted in psychosis. **Methods:** We carried out a case study of a middle-aged patient who presented with new-onset psychosis associated with a space-occupying lesion localized in the right superior colliculus/periaqueductal gray. The study sought to investigate potential connectivity deficits related to the lesion by the use of diffusion tensor imaging and resting-state functional magnetic resonance imaging. To this aim, we generated a functional connectivity map of the patient's brain, centered on the lesion area, and compared this map with the corresponding map of 10 sex- and age-matched control individuals identified from the Max Planck Institute–Leipzig Mind–Brain–Body database. **Results:** Our analysis revealed a discrete area in the right rostral tectum, in the immediate vicinity of the lesion, whose activity is inversely correlated with the activity of left amygdala, whereas left amygdala is functionally associated with select areas of the temporal, parietal, and occipital lobes. Based on a comparative analysis of the patient with 10 control individuals, the lesion has impacted on the connectivity of rostral tectum (superior colliculus/periaqueductal gray) with left amygdala as well as on the connectivity of left amygdala with subcortical and cortical areas. **Conclusions:** The superior colliculus/periaqueductal gray might play important roles in the initiation and perpetuation of psychosis, at least partially through dysregulation of left amygdala activity.

Key words: psychosis/schizophrenia/neural connectivity/resting-state functional MRI/superior colliculus/periaqueductal gray/amygdala

Introduction

In schizophrenia, there is severe dysregulation of anatomical and functional neuronal connectivity among

primary and higher-order brain areas serving distinct functions.^{1,2} This dysregulation has been substantiated on the basis of resting-state activity of broadly distributed functional networks in schizophrenic individuals.² Despite the advances in elucidating such networks, two major questions remain unanswered. First, functional connectivity aberrations that occur in prodromal stages of psychosis remain occult. Second, the precise neural pathways underlying psychosis have yet to be identified; despite that certain structures, such as the hippocampus, exhibit profound structural and functional abnormalities in psychosis,³ it is unknown whether these deficits underlie psychosis or they constitute the sequela of generalized and lasting brain dysfunction.

It is well known that in both prodromal and clinically overt psychosis, there is impairment of saccadic eye movements^{4–6}; the latter are controlled cortically by the frontal eye field and subcortically by the superior colliculus (SC).⁷ The SC consists of multiple layers, each with distinct inputs and outputs.^{8,9} The SC receives inputs from retinal ganglion cells,¹⁰ cortical areas (visual, auditory, motor, prefrontal),^{9,11,12} locus coeruleus¹³ and its efferents project to cortex,⁸ substantia nigra pars compacta,¹⁴ amygdala through the pulvinar,¹⁵ parabigeminal nucleus,^{9,16,17} lateral posterior thalamic nucleus,^{9,17,18} and brainstem nuclei.⁹ The SC, besides being an integral part of the visual pathway,⁷ constitutes a cross-modal integration center capable of guiding motor behaviors in response to external stimuli.^{19–21} In particular, SC excitation can drive fear, anxiety, and defensive behaviors^{8,9,11,16–18,22–25}; this is largely mediated by excitatory collicular projections to amygdala through the parabigeminal nucleus^{9,16,17} or through the thalamus.¹⁸ In addition, the closely associated periaqueductal gray (PAG), which is directly connected

to SC,⁹ plays essential roles in fear expression and defensive behavior^{26–28} and is also connected to amygdala.^{28–30} Of note, amygdala is indispensable for escape from impending threats.³¹ However, despite elegant research in animal models, schizophrenic phenotypes cannot be fully reproduced with the existing behavioral paradigms.^{32,33}

Herein, we report a case study of a middle-aged individual who presented with subacute psychosis associated with a space-occupying lesion localized in the rostral tectum, within the right SC and PAG. Our functional connectivity analysis implicates the SC, PAG and left amygdala in psychosis. Although our case study cannot test causality, it is the first study to provide compelling evidence for an association of SC/PAG with a psychotic behavioral phenotype in the absence of any neurologic disability. It is, however, the second study that reports an association of a tectal lesion with psychosis, with the first one described in a young woman who presented with psychosis as a result of a quadrigeminal plate lipoma.³⁴

Methods

Magnetic Resonance Imaging Acquisition Parameters

Magnetic resonance data from the patient were acquired using Philips Medical Systems Achieva-3T. T1 weighted images were acquired with the following parameters: field of view (FoV) = 24.0 cm, voxel size = $0.94 \times 0.94 \times 1.20$ mm³, slice thickness = 1.20 mm, flip angle (FA) = 10°, time repetition (TR) = 6.23 s, time echo (TE) = 3.00 s. Images of diffusion tensor imaging (DTI) were acquired using echo-planar imaging (EPI) with parameters: FoV = 22.4 cm, voxel size = $1.75 \times 1.75 \times 2.0$ mm³, slice thickness = 2.00 mm, FA = 90°, TR = 7.39 s, TE = 71 ms, number of averages = 1, $b = 1000$ s/mm², number of directions = 30. Functional images were acquired using EPI sensitive to blood oxygenation with parameters: FoV = 24.0 cm, voxel size = $3 \times 3 \times 3$ mm³, slice thickness = 3.00 mm, FA = 90°, TR = 2.49 s, TE = 30 ms, and 6-minute scan time length. In the control group, data were acquired using Siemens Verio-3T. Functional images (EPI) were acquired with parameters: FoV = 20.2 cm, voxel size = $2.3 \times 2.3 \times 2.3$ mm³, slice thickness = 2.30 mm, FA = 69°, TR = 1.40 s, TE = 30 ms, and 15 minutes 30 seconds scan time length.³⁵

Diffusion Tensor Imaging Analysis

All analyses were conducted using FSL software (version 5.0). The DTI data were preprocessed to correct for eddy current-induced distortions and then brain-extracted to isolate the brain structures. Diffusion tensors reconstruction and diffusion parameters were obtained using BEDPOSTX tool with three fiber orientations per voxel, to model crossing fibers.³⁶ To proceed with tractography, we first registered a structural T1 sequence to the DTI sequence using a general 3D-to-3D linear

(affine) transformation with 12 degrees of freedom.³⁷ We then selected manually, using fsleyes tool, a seed region around superior colliculus in the T1 sequence and used PROBTRACKX tool on BEDPOSTX output to reconstruct fiber bundles.

In [figure 3B](#), the principal direction of diffusion is displayed at each voxel. Fractional anisotropy is a good marker of white matter integrity and fractional anisotropy values modulate the brightness of the vectors. When white matter is intact anisotropic voxels appear bright, whereas loss of white matter structure gives low fractional anisotropy values and thus low brightness vectors.

Resting-State Functional Magnetic Resonance Imaging Analysis

Resting-state functional magnetic resonance imaging (rs-fMRI) analysis was conducted using CONN toolbox³⁸ and SPM12 (<https://www.fil.ion.ucl.ac.uk/spm/>), unless otherwise stated. The structural T1 scan was brain-extracted using FSL and then coregistered to functional images. Structural and functional images were mapped to the standardized Montreal Neurological Institute (MNI) space. FMRI data were preprocessed to apply motion estimation and correction, slice timing correction, outlier detection, and spatial Gaussian smoothing. FMRI data denoising was performed with high-pass filtering to remove low-frequency noise. First-level seed-based connectivity analysis was performed using correlation coefficient, r . The seed regions, which are the left or right amygdala and intracalcarine cortex (ICC), were selected on Harvard–Oxford atlas.³⁹ For each seed region, a correlation map was evaluated by computing r between the seed Blood Oxygen Level Dependent (BOLD) signal and the BOLD signal of all brain voxels.

To identify brain regions with significantly altered functional connectivity in the patient, we performed a seed-to-voxel second-level analysis. We compared our patient (60 years old) with a group of 10 sex- and age-matched (three aged 55–60 years and seven aged 60–65 years) healthy control individuals from the publicly available Max Planck Institute–Leipzig Mind–Brain–Body data set.^{35,40} We tested for differences using a two-sample t -test and set the significance threshold at a $P < .001$.

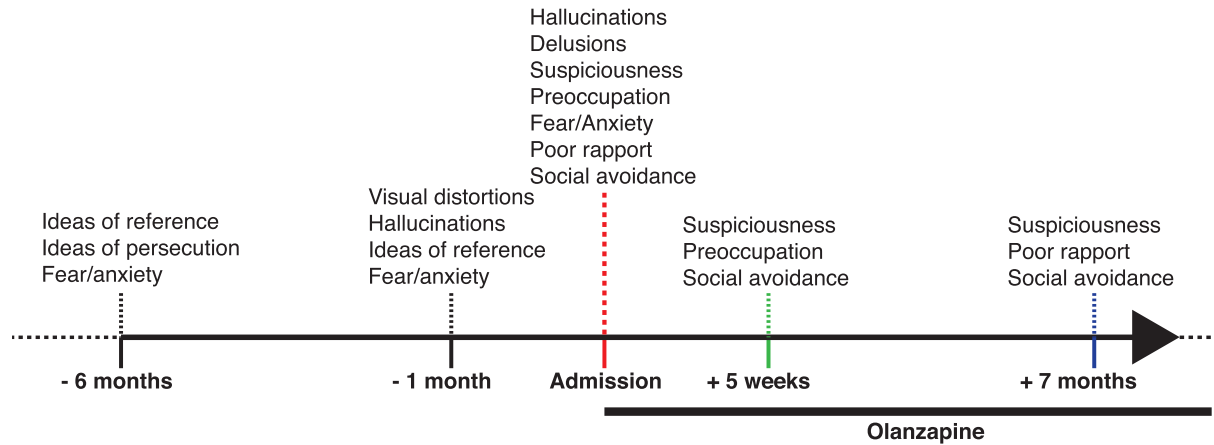
For cluster analysis, we performed a whole brain seed-to-voxel analysis, applying cluster-based thresholding for multiple comparisons correction (significance level $P < .05$, false discovery rate corrected). Left amygdala was selected as the seed region of interest.

Results

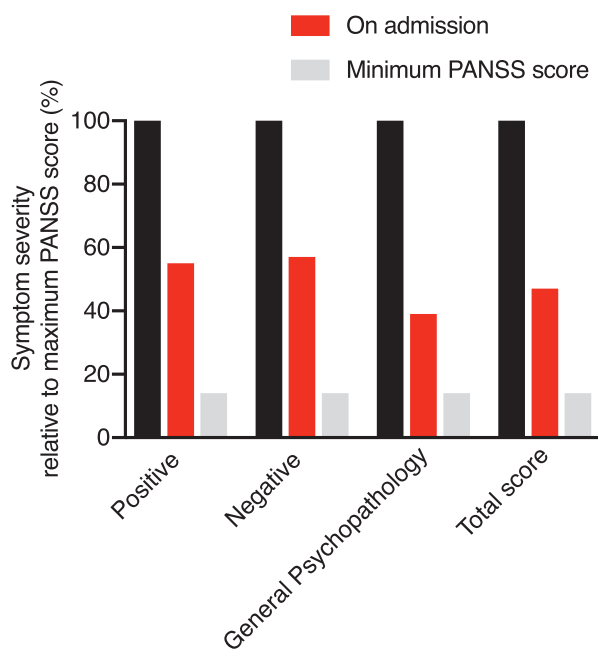
New-Onset Psychosis Associated With a Lesion Localized in the Rostral Tectum

A 60-year-old female presented with psychosis that had insidiously progressed over several months ([figure 1A](#)). In

A Temporal pattern of the psychiatric syndrome progression



B



C

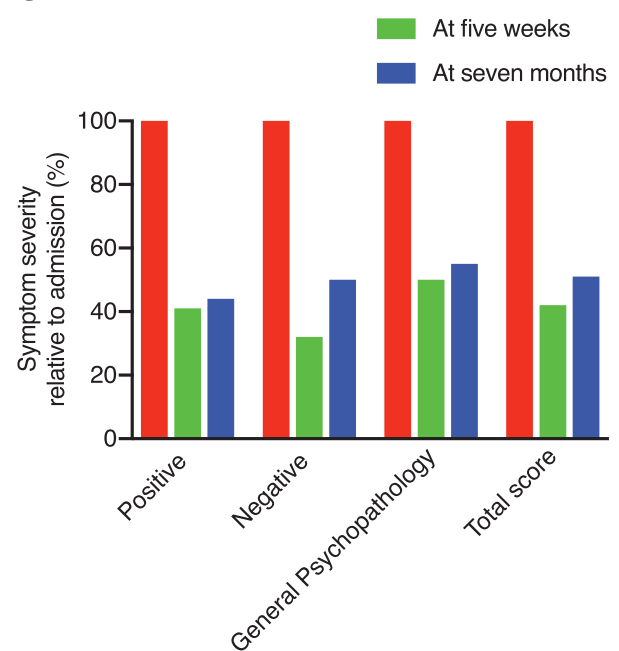


Fig. 1. The course of the patient's psychiatric syndrome. (A) Timeline of the psychiatric syndrome, which emerged 6 mo before presentation and gradually progressed with the manifestation of a hallucinatory behavior. Olanzapine was initiated on admission and continued thereafter. (B, C) The 30-item PANSS was administered at three time points: on admission, at 5 wk, and at 7 mo of olanzapine treatment. Each of the positive, negative, and general psychopathology symptoms is graded (1–7), and the corresponding scores are calculated for the three time points. (B) Quantification of psychosis symptoms on admission relative to maximum pathology (maximum PANSS scores—total: 210; positive: 49; negative: 49; general psychopathology: 112—are set at 100% and the admission scores are presented as a percentage of the corresponding maximum scores). (C) Quantification of psychosis symptoms at 5 wk and at 7 mo of olanzapine treatment presented as a percentage of admission PANSS scores.

greater detail, 6 months ago the patient started to have ideas of reference and persecution and on several occasions over the next months she experienced visual distortions—perceived the faces of people as “yellow- and strange-looking.” The last few weeks prior to admission the patient increasingly experienced frightening auditory and visual hallucinations that resulted in disorganized behavior and severe decline in daily functioning. On admission, the patient presented fearful, perplexed, and had

a high degree of distrust and thought broadcasting. The severity of psychosis was assessed with the Positive And Negative Syndrome Scale (PANSS)⁴¹ (figure 1B).

Of note, the patient did not sustain any alteration in the level of consciousness, seizures, visual acuity or hearing deficits, or constitutional symptoms. No misidentification of faces, places, or objects was noticed. No sleep-arousal alterations were present. Furthermore, symptoms or signs of autonomic dysfunction were absent. The

patient's home medications included olmesartan and omeprazole. A detailed neurologic examination was unremarkable. The remainder of the physical examination was unrevealing.

The lack of prior psychiatric history prompted us to pursue a thorough differential diagnosis that included metabolic derangements, medications, drug abuse, autoimmune/paraneoplastic encephalitis, central nervous system infections, space-occupying lesions, epilepsy, migraine aura, major depression with psychosis, vascular and neurodegenerative disorders. Initial evaluation with routine laboratory testing and urine drug screening was noncontributory. Serologic testing for human immunodeficiency virus-1 and -2 and hepatitis B and C was negative. The general and immunologic examination of cerebrospinal fluid revealed no abnormalities, whereas polymerase chain reaction and culture for various pathogens turned out negative. Electroencephalographic study did not reveal abnormal activity patterns indicative of local or generalized brain dysfunction. Moreover, there were no overt cognitive deficits observed (30/30 in Mini-Mental State Examination administered a few weeks after olanzapine treatment).

Brain MRI revealed a well-circumscribed lesion in the tectum (dorsal midbrain), consistent with a low-grade glioma, which localized in the right SC and PAG

and slightly displaced the cerebral aqueduct without causing obstructive hydrocephalus (figures 2A–2C). The inferior colliculus is spared as evidenced radiologically (figure 2D) and clinically by the absence of trochlear nerve palsy. Importantly, all structures lying ventrally or rostrally appeared intact, in agreement with the absence of neurologic signs.

To investigate other potential causes of psychosis, an extensive work-up for underlying systemic illnesses with inflammation markers, immunoglobulins, complement factors, antinuclear and extractable nuclear antigen antibodies, and venereal disease research laboratory test turned out negative. A work-up for an underlying malignancy was unrevealing. To further investigate for autoimmune psychosis, the patient's serum was analyzed for antibodies directed against *N*-methyl-D-aspartate receptor, α -amino-3-hydroxy-5-methyl-4-isoxazolepropionic acid receptor, voltage-gated potassium channels, contactin-associated protein 2, and leucine-rich glioma inactivated 1, which have been previously detected in a subset of patients with psychosis.^{42,43} No such immunoreactivity was detected in the patient's serum.

Taken together, the absence of other precipitating factors, the exclusion of autoimmune encephalitis,^{44,45} and the temporal course of psychiatric manifestations point toward a psychotic syndrome associated with

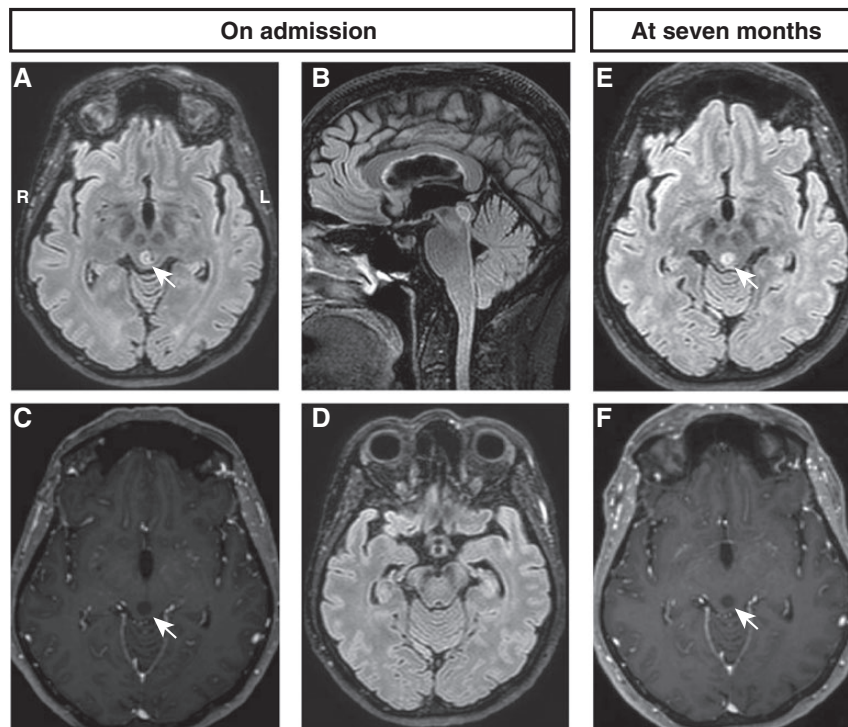


Fig. 2. Brain magnetic resonance imaging reveals a lesion localized in the right half of the rostral tectum. (A, B) Fluid-attenuated inversion recovery (FLAIR) images reveal a space-occupying lesion within the right superior colliculus and periaqueductal gray (A: axial, B: sagittal). The lesion displaces the cerebral aqueduct without affecting the patency of the ventricular system. (C) Axial T1-weighted image following gadolinium administration reveals no enhancement of the lesion. (D) Axial FLAIR image at the level of the inferior colliculus reveals sparing of the inferior colliculi. (E, F) Axial MRI images acquired 7 mo later reveal no size alterations or contrast enhancement of the lesion (E: FLAIR; F: T1-weighted sequence with gadolinium). R and L denote the right and left side, respectively.

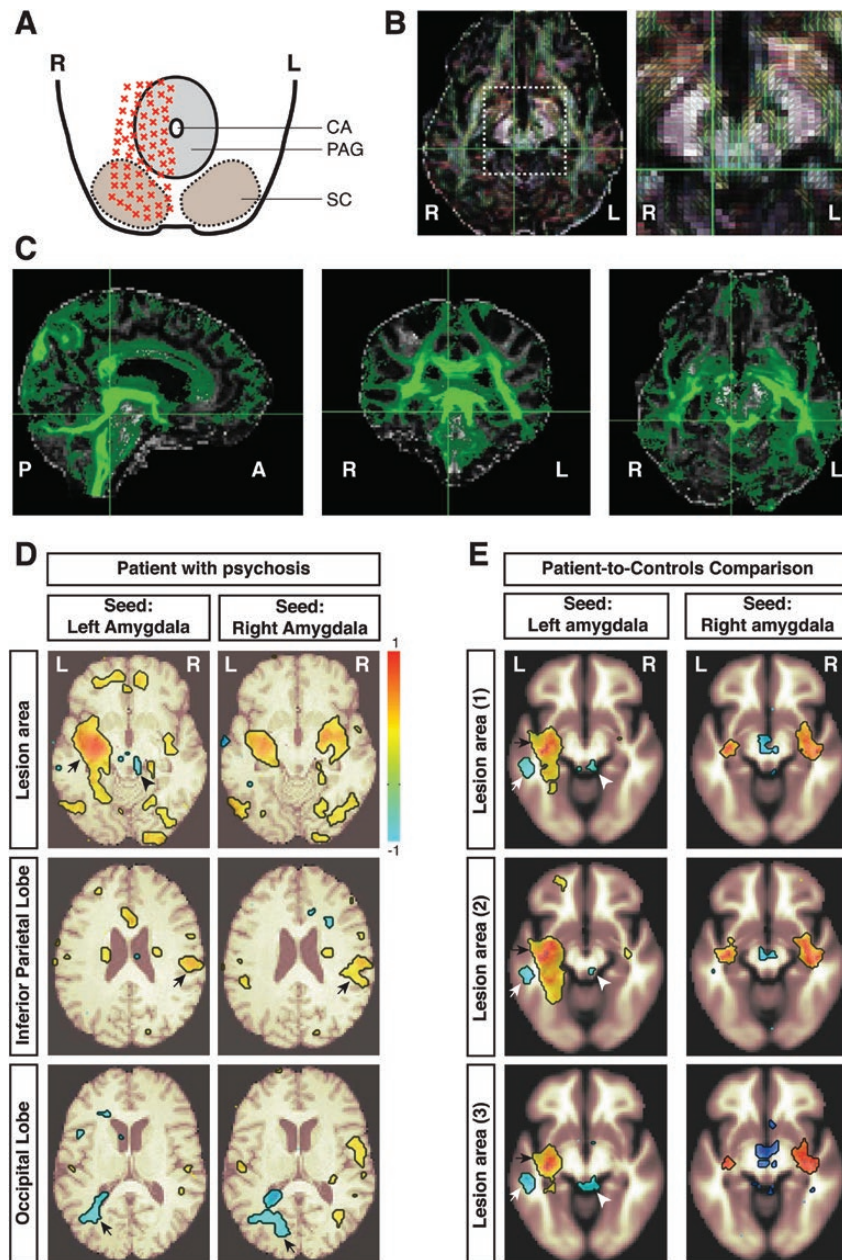


Fig. 3. A structural and functional brain map centered on the tectal area displaying the lesion. (A) Schematic depiction of the lesion (red crosses), which occupies the right superior colliculus (SC) and right half of periaqueductal gray (PAG) abutting the cerebral aqueduct (CA). (B) Fractional anisotropy map at the level of the lesion reveals no gross white matter differences between the left (no lesion) and the right (lesion) side; right panel shows a zoomed-in view of the area surrounded by the rectangle. (C) Fiber tractography traces the long-range afferent and efferent projections of rostral tectum, which connect it to the visual pathway (the cuneus, in particular around calcarine fissure [primary visual cortex] and parieto-occipital sulcus [higher-order visual cortex], and the lower part of precuneus [higher-order visual processing]), the middle temporal gyrus, the cerebellum, the splenium of corpus callosum, and the medulla and spinal cord. (D) Seed-to-voxel analysis of fMRI, using as a seed the left or right amygdala, revealed brain areas functionally associated with the seed positively (correlated, red) or negatively (anticorrelated, blue). Note an area in right SC adjacent to the lesion (black arrowhead) that displays anticorrelated activity with left amygdala, but not right amygdala. Correlated activity is revealed between left amygdala and structures of the left temporal lobe including the hippocampus, the parahippocampal gyrus, the planum polare, and the superior temporal gyrus (top row, black arrow). Both amygdalae display correlated activity with the right inferior parietal lobe (middle row, black arrow) and anticorrelated activity with the left occipital lobe (bottom row, black arrow). (E) Functional connectivity alterations in the patient compared to controls. Seed-to-voxel second-level correlation analysis revealed reduced connectivity between an area surrounding the lesion (white arrowhead) and left amygdala and between left amygdala and the posterior division of the left middle temporal gyrus (white arrow) in the patient. Increased connectivity in the patient is revealed between left amygdala and distinct areas of the left cerebral hemisphere (black arrow), including the planum polare, the superior temporal gyrus, the hippocampus, the parahippocampal gyrus (posterior division), the temporal occipital fusiform cortex, the lingual gyrus, the putamen, and the insular cortex. Unlike left amygdala, right amygdala does not exhibit similar associations. R and L denote the right and left side, respectively.

the detected lesion. The patient received olanzapine (15 mg/day) with marked symptomatic remission and recovery in daily functioning (figure 1C). On follow-up, the tectal lesion appeared stable (figures 2E and 2F). The efficacy of antipsychotics in ameliorating psychosis associated with underlying pathology has been previously reported.^{46,47}

Generation of a Structural and Functional Connectivity Map Centered on the Area of the Lesion

We next sought to identify potential connectivity deficits underlying the above-described psychotic syndrome. To visualize the anatomic connectivity of the tectal area displaying the lesion (figure 3A), we implemented DTI. DTI, although incapable of visualizing short-range connections with the exquisite spatial resolution obtained in studies in mice, has allowed the visualization of gross white matter tract abnormalities in schizophrenic individuals.⁴⁸ First, we generated a fractional anisotropy map of the patient's brain that revealed no detectable, to visual inspection, white matter changes resulting from the lesion (figure 3B). Second, we set the rostral tectum as a region of interest and visualized its long-range connectivity; this analysis traced large fiber bundles connecting to the visual pathway (cuneus, precuneus), the temporal lobe, the cerebellum, the splenium of corpus callosum, and the medulla and spinal cord (figure 3C), in consistency with its known connectivity.^{8,9}

Next, to gain insight into the functional connectivity of the area of interest, we performed resting-state functional Magnetic Resonance Imaging (rs-fMRI) and implemented seed-to-voxel correlation analysis. Based on the well-documented connectivity between SC and amygdala and between PAG and amygdala (summarized in the "Introduction" section), we attempted to investigate a potential association of the affected area with the amygdalae using the left or right amygdala as a seed.

Interestingly, this analysis revealed a small area in the right rostral tectum, in close proximity to the lesion, whose activity is inversely correlated with the activity of left amygdala (figure 3D, black arrowhead). Unlike left amygdala, right amygdala does not display a similar functional connection, in keeping with the studies showing that left amygdala is more often implicated, compared with the right one, in the processing of emotional stimuli.⁴⁹ A similar analysis with the left ICC as a seed revealed correlated activity between the tectal area surrounding the lesion and left ICC (data not shown).

Given the functional association of the lesion area with left amygdala, we sought to explore the connectivity of left amygdala with cortical and subcortical areas. Our rs-fMRI analysis revealed that left amygdala displays correlated activity with select areas of the left temporal lobe, whereas both amygdalae exhibit correlated activity with the right parietal lobe and anticorrelated activity with the

left occipital lobe (figure 3D). Therefore, a lesion-induced dysregulation of neuronal activity in the tectum could result in aberrant activity within left amygdala and subsequently in select cortical domains involved in sensory perception.

A Patient-to-Control Comparison Reveals Functional Connectivity Aberrations in the Patient Suffering From Psychosis

To address whether the lesion-associated functional connectivity we uncovered in the patient relates to psychosis, we compared the functional connectivity map of the patient's brain with that of 10 sex- and age-matched control individuals selected from the Max Planck Institute–Leipzig Mind–Brain–Body dataset³⁵ (see [Supplementary Material](#)). This analysis revealed weaker connectivity between the right SC and left amygdala and between left amygdala and part of the left middle temporal gyrus, in the patient compared with controls, whereas increased connectivity was detected in the patient between left amygdala and select areas of the left cerebral hemisphere (figure 3E). It is noteworthy that the areas of the left temporal lobe that display positive functional association with left amygdala (figure 3D, left upper panel) are the same with the ones that exhibit higher connectivity with left amygdala in the patient compared with controls (figure 3E, black arrows). This constellation of functional connectivity associations supports a role of left amygdala in the patient's psychotic syndrome.

To further explore lesion-induced connectivity perturbations, we performed cluster analysis. Using left amygdala as a seed, we extracted the brain areas that display increased (figure 4A) or decreased connectivity (figure 4B) with left amygdala in the patient compared with controls. These data are in line with our previous analysis (figure 3E).

Discussion

This study provides indirect, yet intriguing, evidence for the role played by the rostral tectum in the pathophysiology of psychosis. Although we cannot address causality, the course of psychosis, the exclusion of other causes, and the evidence for the existence of a circuit involving an area previously implicated in behavioral derangements in animal models,^{9,11,16–18,26–28,50} which is affected by the lesion, provide support for the pathogenic relevance of this pathway to patient's psychosis. As such, it is the first case study to implicate SC/PAG in a psychotic behavioral phenotype; of note, in the absence of neurologic deficits.

Several studies have reported that ventral midbrain or pontine lesions can cause hallucinosis.^{51–56} The association of tectum with psychosis was first described in an adolescent who suffered from a tectal lipoma and psychosis

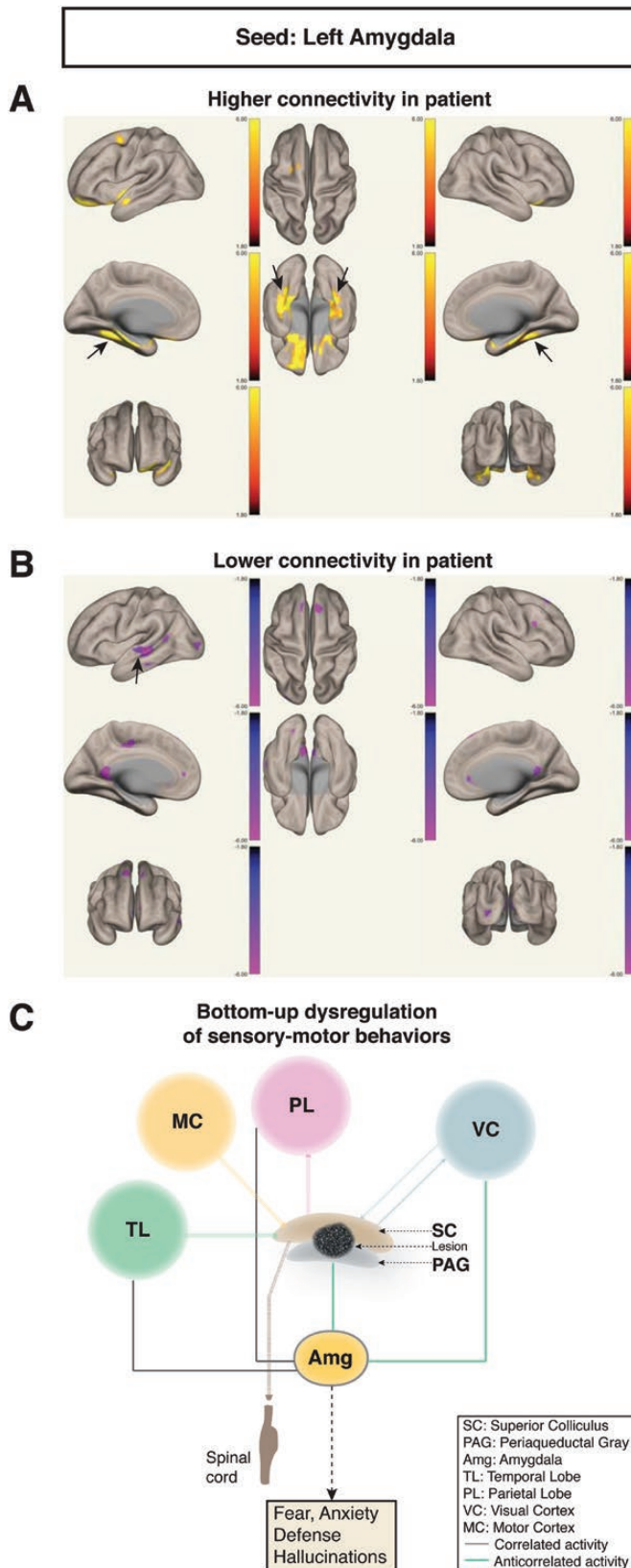


Fig. 4. Functional connectivity perturbations in the patient revealed by cluster analysis. (A, B) Identification of clusters with seed-to-voxel analysis in the patient and controls using as seed the left amygdala. (A) Brain areas that exhibit higher connectivity with left amygdala in the patient compared with

was preceded by headache.³⁴ It has also been illustrated in a study that revealed differences in inferior colliculus size between schizophrenic and healthy individuals.⁵⁷ In our case, psychosis resulted from a lesion restricted within the right SC/PAG (figures 2 and 3A). Although it is well demonstrated that saccades are impaired in psychotic disorders,⁴⁻⁶ our study suggests additional roles for SC in psychosis that relate to positive and negative symptoms and apparently result from aberrant activity of SC/PAG input and output areas (figure 4C). Therefore, SC/PAG may serve as subcortical nodes of a bottom-up circuit that dysfunctions in at least a subset of psychotic patients. With respect to how a unilateral lesion is sufficient to cause psychosis, lateralization of SC function arises as the mechanism most likely to account for this (figure 3D), in line with functional lateralization shown for other brain structures.^{49,58}

Besides positive symptoms, the patient also manifested severe negative symptoms (figure 1), which make up a major factor of morbidity in schizophrenia.^{59,60} A plausible explanation would be that positive symptoms make the patient abstain from social engagement. It is also possible that abnormal functional communication and synchronization with important subcortical hubs in this study (tectum, amygdala) produce abnormal behaviors not normally present in the population (positive symptoms) in addition to behavioral deficits (negative symptoms).⁶⁰

It is known that dopamine receptor blockers possess a central part in the therapeutics of psychosis.⁶¹ Thus, if SC/PAG and amygdala play a role in psychotic disorders, they should modulate dopaminergic signaling. In support of this, there are compelling data for a role of SC in select dopaminergic pathways^{14,62-65} and for altered amygdala-mediated dopaminergic signaling in schizophrenia that may be modified by antipsychotic medications.⁶⁶⁻⁶⁹

Although this study attempts to elucidate important aspects of psychosis pathogenesis, it has certain limitations. First, additional research in large cohorts is

controls: hippocampus–parahippocampal gyrus–posterior temporal fusiform cortex bilaterally (left more than right for all structures) (black arrows) and cerebellum bilaterally. (B) Brain areas that exhibit lower connectivity with left amygdala in the patient compared with controls: vermis, posterior division of the left superior and middle temporal gyri (black arrow), thalamus (left more than right), caudate (right more than left), and right accumbens. The *t*-value statistic is plotted in range of critical *t*-values at 95% (*t*-value of 1.83) and 99.99% (*t*-value of 6.01) percentiles. (C) Schematic illustration of a bottom-up circuit that can lead to emotional perturbations and hallucinations and is modulated by top-down processes mediated by corticofugal projections. In our paradigm, there is anticorrelated activity between an area in rostral tectum spatially associated with the lesion and left amygdala. Given that left amygdala displays distinct functional associations with select cortical domains, a lesion-induced SC/PAG activity dysregulation could release left amygdala activity and alter cortical function.

needed to determine whether the findings of this study generalize to psychotic disorders. Second, our DTI analysis visualizes long-range connectivity and cannot rule out subtle effects or changes to white matter pathways. Third, despite the absence of gross cognitive dysfunction, extensive cognitive assessment was not a major goal of the study and we cannot rule out the presence of cognitive deficits associated with the tectal lesion.

Taken together, our data support the notion that SC/PAG and left amygdala constitute important neural substrates of psychosis through impaired sensorimotor integration⁷⁰ (figure 4C). The findings of our and similar studies in humans in conjunction with studies in animal models could have important ramifications for understanding the neurophysiology of psychosis.

Supplementary Material

Supplementary data are available at *Schizophrenia Bulletin* online.

Funding

N.M. is funded by General Secretariat for Research and Technology (GSRT) and Hellenic Foundation for Research and Innovation (HFRI).

Acknowledgments

We thank Efstathios Vlachakis, MD (Evangelismos Hospital, Athens), for providing neurosurgical consultation and Eirini Pantou, MD, for providing a report of the patient's brain MRI. We also thank Tzartos NeuroDiagnostics (Athens) for providing testing for neuronal autoantibodies at no charge.

Conflict of interest

The authors declare no conflict of interest related to the work presented here.

Ethical requirement statement

All clinical and laboratory procedures were performed according to the ethical principles for human medical research established by the Declaration of Helsinki (1964 and subsequent amendments) and in line with the "Code of Medical Ethics" (Article 62 N. 2071/1992) and "The Rights of the Nosocomial Patient" (Article 47 N. 2071/1992) of the Greek National Council on Medical Ethics (Article 61 N. 2071/1992) as well as in accordance with the institutional policies of Aiginition Hospital. The Inspectorate of Aiginition Hospital approved the

case study (approval number: 535). The patient signed a written informed consent after having a significant amelioration of psychiatric symptoms and recovery of daily functioning while on olanzapine treatment.

References

1. Burns J, Job D, Bastin ME, et al. Structural disconnectivity in schizophrenia: a diffusion tensor magnetic resonance imaging study. *Br J Psychiatry*. 2003;182:439–443.
2. Woodward ND, Rogers B, Heckers S. Functional resting-state networks are differentially affected in schizophrenia. *Schizophr Res*. 2011;130(1–3):86–93.
3. Schobel SA, Chaudhury NH, Khan UA, et al. Imaging patients with psychosis and a mouse model establishes a spreading pattern of hippocampal dysfunction and implicates glutamate as a driver. *Neuron*. 2013;78(1):81–93.
4. Gooding DC, Mohapatra L, Shea HB. Temporal stability of saccadic task performance in schizophrenia and bipolar patients. *Psychol Med*. 2004;34(5):921–932.
5. Myles JB, Rossell SL, Phillipou A, Thomas E, Gurvich C. Insights to the schizophrenia continuum: a systematic review of saccadic eye movements in schizotypy and biological relatives of schizophrenia patients. *Neurosci Biobehav Rev*. 2017;72:278–300.
6. Obyedkov I, Skuhareuskaya M, Skugarevsky O, et al. Saccadic eye movements in different dimensions of schizophrenia and in clinical high-risk state for psychosis. *BMC Psychiatry*. 2019;19(1):110.
7. Gandhi NJ, Katnani HA. Motor functions of the superior colliculus. *Annu Rev Neurosci*. 2011;34:205–231.
8. Basso MA, May PJ. Circuits for action and cognition: a view from the superior colliculus. *Annu Rev Vis Sci*. 2017;3:197–226.
9. Zingg B, Chou XL, Zhang ZG, et al. AAV-mediated anterograde transsynaptic tagging: mapping corticocollicular input-defined neural pathways for defense behaviors. *Neuron*. 2017;93(1):33–47.
10. Ellis EM, Gauvain G, Sivyer B, Murphy GJ. Shared and distinct retinal input to the mouse superior colliculus and dorsal lateral geniculate nucleus. *J Neurophysiol*. 2016;116(2):602–610.
11. Liang F, Xiong XR, Zingg B, Ji XY, Zhang LI, Tao HW. Sensory cortical control of a visually induced arrest behavior via corticotectal projections. *Neuron*. 2015;86(3):755–767.
12. Hu F, Kamigaki T, Zhang Z, Zhang S, Dan U, Dan Y. Prefrontal corticotectal neurons enhance visual processing through the superior colliculus and pulvinar thalamus. *Neuron*. 2019;104(6):1141–1152.e4.
13. Li L, Feng X, Zhou Z, et al. Stress accelerates defensive responses to looming in mice and involves a locus coeruleus-superior colliculus projection. *Curr Biol*. 2018;28(6):859–871.e5.
14. Comoli E, Coizet V, Boyes J, et al. A direct projection from superior colliculus to substantia nigra for detecting salient visual events. *Nat Neurosci*. 2003;6(9):974–980.
15. Rafal RD, Koller K, Bultitude JH, et al. Connectivity between the superior colliculus and the amygdala in humans and macaque monkeys: virtual dissection with probabilistic DTI tractography. *J Neurophysiol*. 2015;114(3):1947–1962.

16. Shang C, Liu Z, Chen Z, et al. A parvalbumin-positive excitatory visual pathway to trigger fear responses in mice. *Science*. 2015;348(6242):1472–1477.
17. Shang C, Chen Z, Liu A, et al. Divergent midbrain circuits orchestrate escape and freezing responses to looming stimuli in mice. *Nat Commun*. 2018;9(1):1232.
18. Wei P, Liu N, Zhang Z, et al. Processing of visually evoked innate fear by a non-canonical thalamic pathway. *Nat Commun*. 2015;6:6756.
19. Alvarado JC, Stanford TR, Rowland BA, Vaughan JW, Stein BE. Multisensory integration in the superior colliculus requires synergy among corticocollicular inputs. *J Neurosci*. 2009;29(20):6580–6592.
20. Ghose D, Maier A, Nidiffer A, Wallace MT. Multisensory response modulation in the superficial layers of the superior colliculus. *J Neurosci*. 2014;34(12):4332–4344.
21. Ito S, Feldheim DA. The mouse superior colliculus: an emerging model for studying circuit formation and function. *Front Neural Circuits*. 2018;12:10.
22. Sahibzada N, Dean P, Redgrave P. Movements resembling orientation or avoidance elicited by electrical stimulation of the superior colliculus in rats. *J Neurosci*. 1986;6(3):723–733.
23. Cohen JD, Castro-Alamancos MA. Neural correlates of active avoidance behavior in superior colliculus. *J Neurosci*. 2010;30(25):8502–8511.
24. Dean P, Mitchell IJ, Redgrave P. Responses resembling defensive behaviour produced by microinjection of glutamate into superior colliculus of rats. *Neuroscience*. 1988;24(2):501–510.
25. DesJardin JT, Holmes AL, Forcelli PA, et al. Defense-like behaviors evoked by pharmacological disinhibition of the superior colliculus in the primate. *J Neurosci*. 2013;33(1):150–155.
26. Koutsikou S, Watson TC, Crook JJ, et al. The periaqueductal gray orchestrates sensory and motor circuits at multiple levels of the neuraxis. *J Neurosci*. 2015;35(42):14132–14147.
27. Deng H, Xiao X, Wang Z. Periaqueductal gray neuronal activities underlie different aspects of defensive behaviors. *J Neurosci*. 2016;36(29):7580–7588.
28. Tovote P, Esposito MS, Botta P, et al. Midbrain circuits for defensive behaviour. *Nature*. 2016;534(7606):206–212.
29. da Costa Gomez TM, Behbehani MM. An electrophysiological characterization of the projection from the central nucleus of the amygdala to the periaqueductal gray of the rat: the role of opioid receptors. *Brain Res*. 1995;689(1):21–31.
30. Da Costa Gomez TM, Chandler SD, Behbehani MM. The role of the basolateral nucleus of the amygdala in the pathway between the amygdala and the midbrain periaqueductal gray in the rat. *Neurosci Lett*. 1996;214(1):5–8.
31. Terburg D, Scheggia D, Triana Del Rio R, et al. The basolateral amygdala is essential for rapid escape: a human and rodent study. *Cell*. 2018;175(3):723–735.e16.
32. Waters F, Fernyhough C. Hallucinations: a systematic review of points of similarity and difference across diagnostic classes. *Schizophr Bull*. 2017;43(1):32–43.
33. Ford JM. Current approaches to studying hallucinations: overcoming barriers to progress. *Schizophr Bull*. 2017;43(1):21–23.
34. Das S, Saini M, Dhyani M, Gupta R. Quadrigeminal plate lipoma presenting with psychosis: a case report with review of literature. *Iran J Psychiatry*. 2015;10(4):288–292.
35. Babayan A, Erbey M, Kumral D, et al. A mind-brain-body dataset of MRI, EEG, cognition, emotion, and peripheral physiology in young and old adults. *Sci Data*. 2019;6:180308.
36. Behrens TE, Berg HJ, Jbabdi S, Rushworth MF, Woolrich MW. Probabilistic diffusion tractography with multiple fibre orientations: what can we gain? *Neuroimage*. 2007;34(1):144–155.
37. Jenkinson M, Smith S. A global optimisation method for robust affine registration of brain images. *Med Image Anal*. 2001;5(2):143–156.
38. Whitfield-Gabrieli S, Nieto-Castanon A. Conn: a functional connectivity toolbox for correlated and anticorrelated brain networks. *Brain Connect*. 2012;2(3):125–141.
39. Rademacher J, Galaburda AM, Kennedy DN, Filipek PA, Caviness VS Jr. Human cerebral cortex: localization, parcellation, and morphometry with magnetic resonance imaging. *J Cogn Neurosci*. 1992;4(4):352–374.
40. Mendes N, Oligschläger S, Lauckner ME, et al. A functional connectome phenotyping dataset including cognitive state and personality measures. *Sci Data*. 2019;6:180307.
41. Kay SR, Fiszbein A, Opler LA. The Positive and Negative Syndrome Scale (PANSS) for schizophrenia. *Schizophr Bull*. 1987;13(2):261–276.
42. Pathmanandavel K, Starling J, Dale RC, Brilot F. Autoantibodies and the immune hypothesis in psychotic brain diseases: challenges and perspectives. *Clin Dev Immunol*. 2013;2013:257184.
43. Schou MB, Sæther SG, Drange OK, et al. The significance of anti-neuronal antibodies for acute psychiatric disorders: a retrospective case-controlled study. *BMC Neurosci*. 2018;19(1):68.
44. Graus F, Titulaer MJ, Balu R, et al. A clinical approach to diagnosis of autoimmune encephalitis. *Lancet Neurol*. 2016;15(4):391–404.
45. Zuliani L, Graus F, Giometto B, Bien C, Vincent A. Central nervous system neuronal surface antibody associated syndromes: review and guidelines for recognition. *J Neurol Neurosurg Psychiatry*. 2012;83(6):638–645.
46. Spiegel D, Barber J, Somova M. A potential case of peduncular hallucinosis treated successfully with olanzapine. *Clin Schizophr Relat Psychoses*. 2011;5(1):50–53.
47. Talih FR. A probable case of peduncular hallucinosis secondary to a cerebral peduncular lesion successfully treated with an atypical antipsychotic. *Innov Clin Neurosci*. 2013;10(5–6):28–31.
48. Kubicki M, McCarley R, Westin CF, et al. A review of diffusion tensor imaging studies in schizophrenia. *J Psychiatr Res*. 2007;41(1–2):15–30.
49. Baas D, Aleman A, Kahn RS. Lateralization of amygdala activation: a systematic review of functional neuroimaging studies. *Brain Res Rev*. 2004;45(2):96–103.
50. Brandão ML, Troncoso AC, de Souza Silva MA, Huston JP. The relevance of neuronal substrates of defense in the midbrain tectum to anxiety and stress: empirical and conceptual considerations. *Eur J Pharmacol*. 2003;463(1–3):225–233.
51. Minabe Y, Kadono Y, Kurachi M. A schizophrenic syndrome associated with a midbrain tegmental lesion. *Biol Psychiatry*. 1990;27(6):661–663.
52. Benke T. Peduncular hallucinosis: a syndrome of impaired reality monitoring. *J Neurol*. 2006;253(12):1561–1571.
53. Penney L, Galarneau D. Peduncular hallucinosis: a case report. *Ochsner J*. 2014;14(3):450–452.
54. McMurtray A, Tseng B, Diaz N, Chung J, Mehta B, Saito E. Acute psychosis associated with subcortical stroke: comparison between basal ganglia and mid-brain lesions. *Case Rep Neurol Med*. 2014;2014:428425.

55. Kronenburg A, Spliet WG, Broekman M, Robe P. Locus coeruleus syndrome as a complication of tectal surgery. *BMJ Case Rep.* 2015;2015:bcr2014207018. doi:10.1136/bcr-2014-207018.
56. Geddes MR, Tie Y, Gabrieli JD, McGinnis SM, Golby AJ, Whitfield-Gabrieli S. Altered functional connectivity in lesional peduncular hallucinosis with REM sleep behavior disorder. *Cortex.* 2016;74:96–106.
57. Kang DH, Kwon KW, Gu BM, Choi JS, Jang JH, Kwon JS. Structural abnormalities of the right inferior colliculus in schizophrenia. *Psychiatry Res Neuroimaging.* 2008;164(2):160–165.
58. Jung YH, Shin JE, Lee YI, Jang JH, Jo HJ, Choi SH. Altered amygdala resting-state functional connectivity and hemispheric asymmetry in patients with social anxiety disorder. *Front Psychiatry.* 2018;9:164.
59. McCutcheon RA, Reis Marques T, Howes OD. Schizophrenia – an overview. *JAMA Psychiatry.* 2020;77(2):201–210.
60. Galderisi S, Mucci A, Buchanan RW, Arango C. Negative symptoms of schizophrenia: new developments and unanswered research questions. *Lancet Psychiatry.* 2018;5(8):664–677.
61. Kaar SJ, Natesan S, McCutcheon R, Howes OD. Antipsychotics: mechanisms underlying clinical response and side-effects and novel treatment approaches based on pathophysiology. [Epub ahead of 9 July 2019] *Neuropharmacology.* 2019:107704. doi:10.1016/j.neuropharm.2019.107704
62. Bertram C, Dahan L, Boorman LW, et al. Cortical regulation of dopaminergic neurons: role of the midbrain superior colliculus. *J Neurophysiol.* 2014;111(4):755–767.
63. Bolton AD, Murata Y, Kirchner R, et al. A diencephalic dopamine source provides input to the superior colliculus, where D1 and D2 receptors segregate to distinct functional zones. *Cell Rep.* 2015;13(5):1003–1015.
64. Muthuraju S, Talbot T, Brandão ML. Dopamine D2 receptors regulate unconditioned fear in deep layers of the superior colliculus and dorsal periaqueductal gray. *Behav Brain Res.* 2016;297:116–123.
65. Essig J, Felsen G. Warning! Dopaminergic modulation of the superior colliculus. *Trends Neurosci.* 2016;39(1):2–4.
66. Reynolds GP. Increased concentrations and lateral asymmetry of amygdala dopamine in schizophrenia. *Nature.* 1983;305(5934):527–529.
67. Laviolette SR. Dopamine modulation of emotional processing in cortical and subcortical neural circuits: evidence for a final common pathway in schizophrenia? *Schizophr Bull.* 2007;33(4):971–981.
68. Kawano M, Oshibuchi H, Kawano T, et al. Dopamine dynamics during emotional cognitive processing: implications of the specific actions of clozapine compared with haloperidol. *Eur J Pharmacol.* 2016;781:148–156.
69. Artiges E, Leroy C, Dubol M, et al. Striatal and extrastriatal dopamine transporter availability in schizophrenia and its clinical correlates: a voxel-based and high-resolution PET study. *Schizophr Bull.* 2017;43(5):1134–1142.
70. Carment L, Dupin L, Guedj L, et al. Impaired attentional modulation of sensorimotor control and cortical excitability in schizophrenia. *Brain.* 2019;142(7):2149–2164.